[Article ID] 1003- 6326(2002)01- 0016- 05

Decomposition processing and precipitation hardening of rapidly solidified Al-Cr-Y-Zr alloy①

XIAO Yu-de(肖于德)[1], LI Wen-xian(黎文献)[1], LI Wei(李 伟)[2],
LI Song-rui(李松瑞)[1], MA Zheng-qing(马正青)[1]
(1. Department of Materials Science and Engineering, Central South University, Changsha 410083, China;
2. Beijing Electro-mechanical Technology Institute, Beijing 100074, China)

[Abstract] Foil powders of Al-5.0Cr-4.0Y-1.5Zr (%) were prepared by using a multi-stage atomization-rapid solidification powder-making device. The obtained powders were exposed thermally at various temperatures. Variation of microstructures and properties of the alloy powders was investigated by micro-hardness measurement, X-ray diffraction, differential thermal analysis, and transmission electron microscopy with energy disperse X-ray analyses. The results show that cubic $Al_{20}Cr_2Y$ (a= 1.437 nm) and metastable Ll_2 Al_3Zr (FCC, a= 0.405 1 nm) or equilibrium DO_{23} Al_3Zr (tetragonal structure, a= 0.409 1 nm, b= 1.730 nm) are main second phases precipitated from supersaturated solid solution of the rapidly solidified foil powders during thermal exposure. The cubic dispersion precipitates prior to the two other Al_3Zr type intermetallic phases in the course of the decomposition. Precipitation of incoherent $Al_{20}Cr_2Y$ results in softening of foil powder, and coherent Ll_2 Al_3Zr has intensive precipitation strengthening effect. The $Al_{20}Cr_2Y$ phase is structurally stable, but it is prone to coarsen and polygonize above 450 ℃. Both Al_3Zr type intermetallic phases have much smaller coarsening rate than $Al_{20}Cr_2Y$ at temperature higher than 450 ℃. These two phases are able to keep their fine spherical morphologies up to 550 ℃, but Al_3Zr transforms into DO_{23} structure from Ll_2 structure during thermal exposure above 550 ℃.

[Key words] rapid solidification; heat-resistant Al alloy; decomposition behavior; precipitation hardening effect
[CLC number] TG 146.2 [Document code] A

1 INTRODUCTION

For last two decades rapidly solidified Al-Cr-Zr(-Mn) heat-resistant aluminum alloy system has been paid a public attention because of its excellent low and high temperature strength and plasticity, and thermal stability. Main second phases of this alloy are equilibrium phase θ-$Al_{13}Cr_2$ (monoclinic, a= 2.52 nm, b= 0.76 nm, c= 1.10 nm, β= 109°) and metastable Ll_2 Al_3Zr (FCC, a= 0.405 1 nm)[1,2]. A lot of past research work focused on improving structural stability of Ll_2 Al_3Zr by adding some elements such as Ti, Nb, V, Hf and so on, and repelling transformation from Ll_2 to DO_{23} Al_3Zr (tetragonal, a= 0.409 1, b= 1.730 nm) at elevated temperature[3,4]. However, it was ignored to improve the structural stability of the phase θ-$Al_{13}Cr_2$ and its coarsening resistance.

Strengthening phases in the heat-resistant aluminum alloys served at high temperature are required to have not only excellent thermal stability but also enough resistance against Ostwald ripening. Although it is structural stable, θ-$Al_{13}Cr_2$ exhibits large coarsening rate[5], and even develops into lumpish morphology at elevated temperature, which deteriorates the mechanical properties of the materials. Hawk and his co-worker[6] pointed out that main strengthening phase of Al-Cr-Y ternary system was $Al_{20}Cr_2Y$ (cubic, a= 1.437 nm), which is structurally stable and has low ripening rate.

Hence, if adding element yttrium into Al-Cr-Zr system, it is possible to develop a new rapidly solidified aluminum alloy, which possesses improved mechanical properties and heat-resistance. Main objective of this work is to carry out basic study for further development of new heat-resistant aluminum alloy and the emphasis is on investigating decomposition behavior and precipitation hardening effect of the rapidly solidified Al-Cr-Y-Zr aluminum alloy.

2 EXPERIMENTAL

Foil powders were produced by a multi-stage atomization rapid solidification powder-making device and had a melt composition of Al-5.0Cr-4.0Y-1.5Zr (mass fraction, %).

The samples, prepared by choosing the foil powder with less than 100 μm thickness and cutting as square shape (a= 10 mm), were aged at exposure

① [Foundation item] Project (G1999064900- 5) supported by the National Key Program of Basic Research Development of China and project 95-YS- 010 supported by the National Key Program of the 9th Five Year Plan of China
[Received date] 2001- 02- 26; [Accepted date] 2001- 07- 16

temperatures of 250, 300, 350, 400, 450, 500, 550, and 600 ℃, and their hardness was measured by a JMT-3 micro-hardness meter (load= 29.4 N).

The thermal behavior of foil powders in heating process was tested by use of differential thermal analysis (DTA) instrument in Ar atmosphere at the heating rate of 20 ℃/min from room temperature to 800 ℃, Identification of phases and measurement on lattice constant of aluminum matrix of testing samples was carried out using a Simens D500 X-ray diffractometer employing CuK_α radiation at 40 kV and 30 mA. The microstructure were examined in detail with an H800 transmission electronic microscope (TEM) equipped with an energy disperse X-ray analysis (EPSX) detector for compositional analysis. The TEM foil was prepared by twin jet thinning electrolytically in a solution of 25% nitric acid and 75% methanol (volume fraction) at - 40 ℃ and an electrical current of 90 mA.

3 RESULTS AND DISCUSSION

3.1 Differential thermal analysis curve

Differential thermal analysis (DTA) curve of the foil powders is shown in Fig. 1. It seems to indicate that, there are three noticeable endothermic peaks on the curve below melt temperature of 644 ℃, which appear approximately at the temperatures of 375, 429, 559 ℃. According to Refs. [7~ 9] and the following results of X-ray diffraction, those noticeable peaks at three above-mentioned temperature ranges are respectively corresponding to the following different transformations: precipitation of $Al_{20}Cr_2Y$, precipitation of Ll_2 Al_3Zr, and stabilization of Ll_2 Al_3Zr into DO_{23} Al_3Zr.

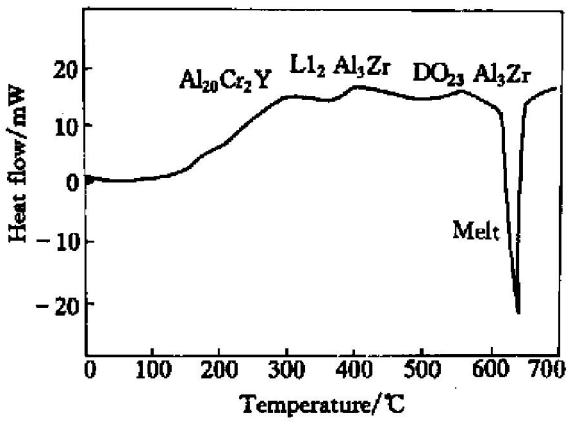

Fig. 1 Differential thermal analysis (DTA) curve of foil powders

3.2 Phase identification and lattice constant measurement by using X-ray diffraction

X-ray diffraction patterns from foil powders after different thermal exposure are shown in Fig. 2.

Under the exist condition of multi-stage rapid solidification, aluminum matrix of the primary foil

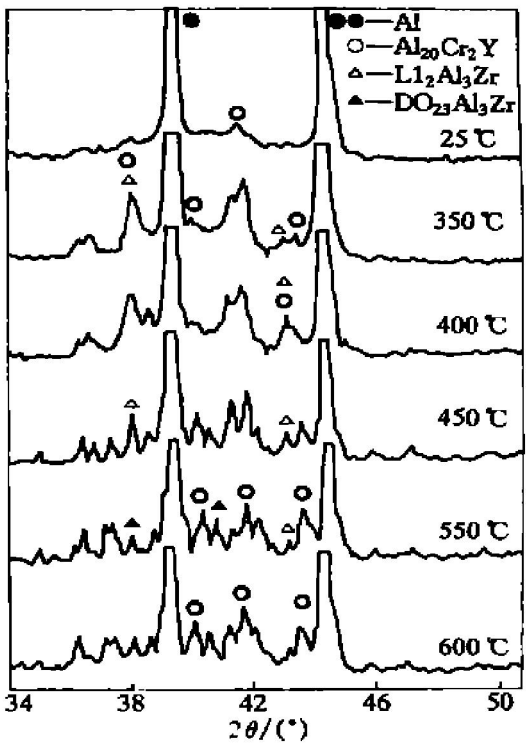

Fig. 2 X-ray diffraction patterns from powders after various thermal exposures for 16 h

powders attains supersaturated solid solution, but perhaps there is a little amount of $Al_{20}Cr_2Y$ phase appearing. The as-quenched Al-5.0Cr-4.0Y-1.5Zr alloy has high thermal stability, and little change is observed until annealing for 10 h below 300 ℃. There is more $Al_{20}Cr_2Y$ phase forming with annealing temperature elevated, but a great amount of $Al_{20}Cr_2Y$ phase precipitates from the aluminum matrix during thermal exposure at medium temperature range of 350 ~ 450 ℃. The phase is so thermally stable as to keep its primary structure up to 600 ℃. Ll_2 Al_3Zr forms at elevated temperature of 400 ℃, but it will transform into DO_{23} Al_3Zr at the temperature higher than 550 ℃. θ-$Al_{13}Cr_2$ is not found in the foil powders of different state, and it indicates that, adding yttrium to the testing alloy will impede θ-$Al_{13}Cr_2$ formation, and make the main precipitated phase rich in chromium element changing from monoclinic $Al_{13}Cr_2$ to cubic $Al_{20}Cr_2Y$.

Variation of lattice constant of the aluminum matrix with exposure time is seen in Fig. 3 during decomposition of the supersaturated solid solution at different temperatures. Generally lattice constant of the aluminum matrix will increase monotonously with $Al_{20}Cr_2Y$ precipitating, and decrease with Al_3Zr doing out of the solid solution[10~12]. Therefore, $Al_{20}Cr_2Y$ phase take the lead in precipitating from the supersaturated solid solution in the course of thermal exposure, and with the increase of exposing temperature elevated, it precipitates more fastly and fully. Al_3Zr phase form after $Al_{20}Cr_2Y$, and only at higher temperature or after longer time, precipitation of Al_3Zr is

dominant. With fuller decomposition of supersaturated solid solution, its lattice constant will be more and more close to that of pure aluminum (a_0 = 0.4049 nm).

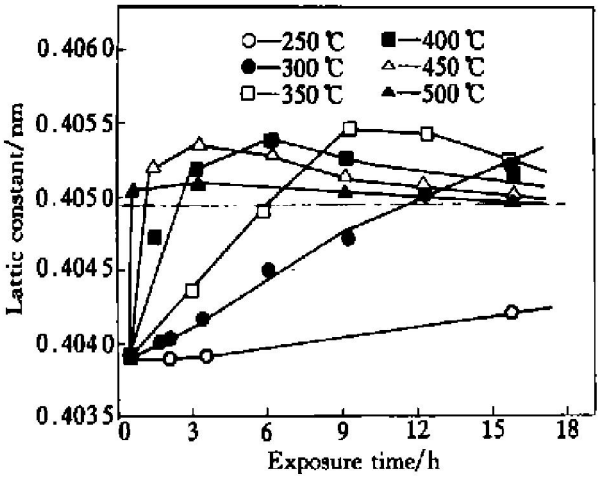

Fig. 3 Variation of lattice constants of aluminum matrix with exposure time

3.3 Annealing hardness curve of foil powders

Fig. 4 indicates variation of hardness of the foil powders soaked at different temperatures with annealing time. The supersaturated solid solution of Al-5.0Cr-4.0Y-1.5Zr has good thermal stability, and decomposes slowly during thermal exposure at low temperature, hence little change of hardness is observed below 250 ℃. Although small amount of $Al_{20}Cr_2Y$ phases form, the powder is supersaturated, and thus its hardness decrease slightly at the temperature of 300 ℃. With increasing temperature, $Al_{20}Cr_2Y$ phase precipitates greatly and the foil powder softens obviously and rapidly, which is especially evident at temperature higher than 550 ℃. It shows that, its dispersion strengthening is not able to offset softening caused by solution reduction due to incoherent nature of $Al_{20}Cr_2Y$ precipitate[12]. The coherent metastable Ll_2 Al_3Zr, will lead to intensive precipitation strengthening effect. Therefore, when thermal exposure above 350 ℃, hardness increases obviously after a stage of reduction and obvious hardening peaks are observed on the annealing hardness curve for suitable time. However, when soaking at higher temperature for longer time hardness of the foil powder decreases significantly, and even above 550 ℃ it is difficult that hardening peak appears on hardness curve.

3.4 Transmission electronic microscope (TEM) microstructures of foil powders

The microstructures of rapidly solidified powder were reported in Refs. [1~8], it was characterized by fine grain aluminum matrix of supersaturated solid solution with little second phases. TEM microstructures of the foil powders after thermal exposure are shown in Fig. 5. The microstructures of foil powder

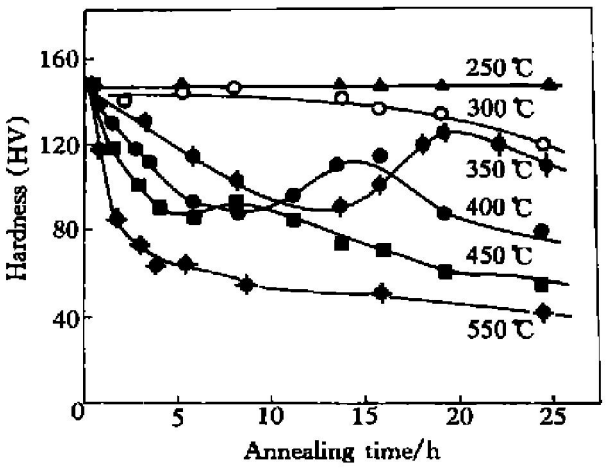

Fig. 4 Relationship curves of hardness of foil powder vs annealing time

in the as-quenched state consist of microdendritic cell structure with a little amount of fine spherical primary intermetallic dispersions mostly along the grain boundary, as shown in Fig. 5(a). There is still only one kind of spherical second phase in the grain interior and boundary of powder exposed at 350 ℃ for 16 h, as shown in Fig. 5(b). Selected area diffraction (SAD) and energy spectra, which are shown in Fig. 6, indicate that the majority of particles are identified as $Al_{20}Cr_2Y$ phase, which is cubic structure with lattice parameter of 1.437 nm. The phase will obviously coarsen and even polygonize with increasing the annealing temperature and time, as shown in Fig. 5(c) and 5(d). Large particles of irregular shape, still identified as $Al_{20}Cr_2Y$ phase, were observed in the sample after thermal exposures at the temperature higher than 450 ℃ for a long time, as shown in Figs. 5(e), 5(f), and Fig. 6, and there is micro-twin structure, as shown in Figs. 6(a) and 6(b), in the lumpish particles of the $Al_{20}Cr_2Y$ phase. On the other hand, there is some spherical particle with much finer size than the $Al_{20}Cr_2Y$ particle in the foil powders in all temperature range above 450 ℃, which was identified as Al_3Zr phase. It implies that both stable (DO_{23} structure) and metastable (Ll_2 structure) Al_3Zr precipitates have much smaller coarsening rate than $Al_{20}Cr_2Y$ at high temperature, it maybe due to extreme low diffusion coefficience of zirconium atom in the aluminum matrix, therefore Al_3Zr is able to keep its fine dimension and spherical shape even up to 550 ℃, as shown in Figs. 5(f) and Fig. 6. However, it should be pointed out that, the cubic phase has more excellent structural thermo-stability and lower ripening rate because of smaller lattice mismatch between $Al_{20}Cr_2Y$ precipitates and aluminum matrix compared with $Al_{13}Cr_2$. Hence, the adding of yttrium into the Al-Cr-Zr alloy is effective to improve its microstructures and its thermal stability. It implies that rapidly solidified Al-Cr-Y-Zr alloy, as compared to that of rapidly solidified Al-Cr-Zr

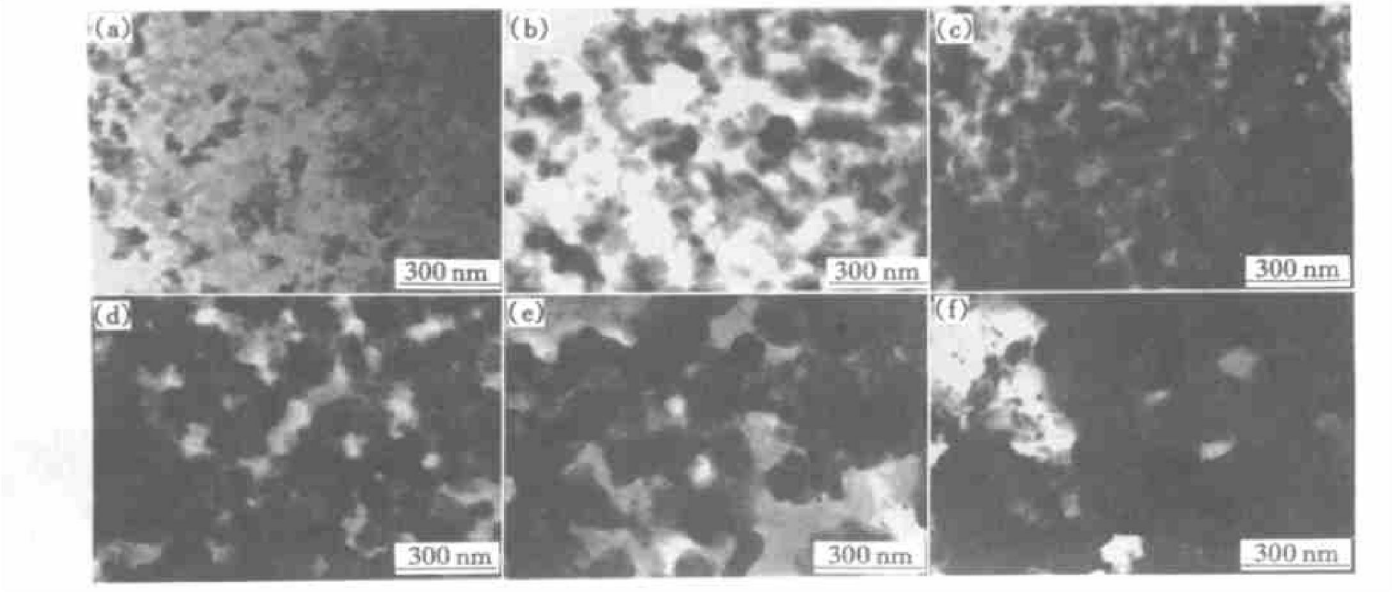

Fig. 5 TEM microstructures of as-solidified foil powder and samples after thermal exposure
(a) —As-solidified; (b) —350 ℃, 16 h; (c) —450 ℃, 16 h; (d) —450 ℃, 32 h;
(e) —500 ℃, 16 h; (f) —550 ℃, 16 h; (g) —600 ℃, 16 h

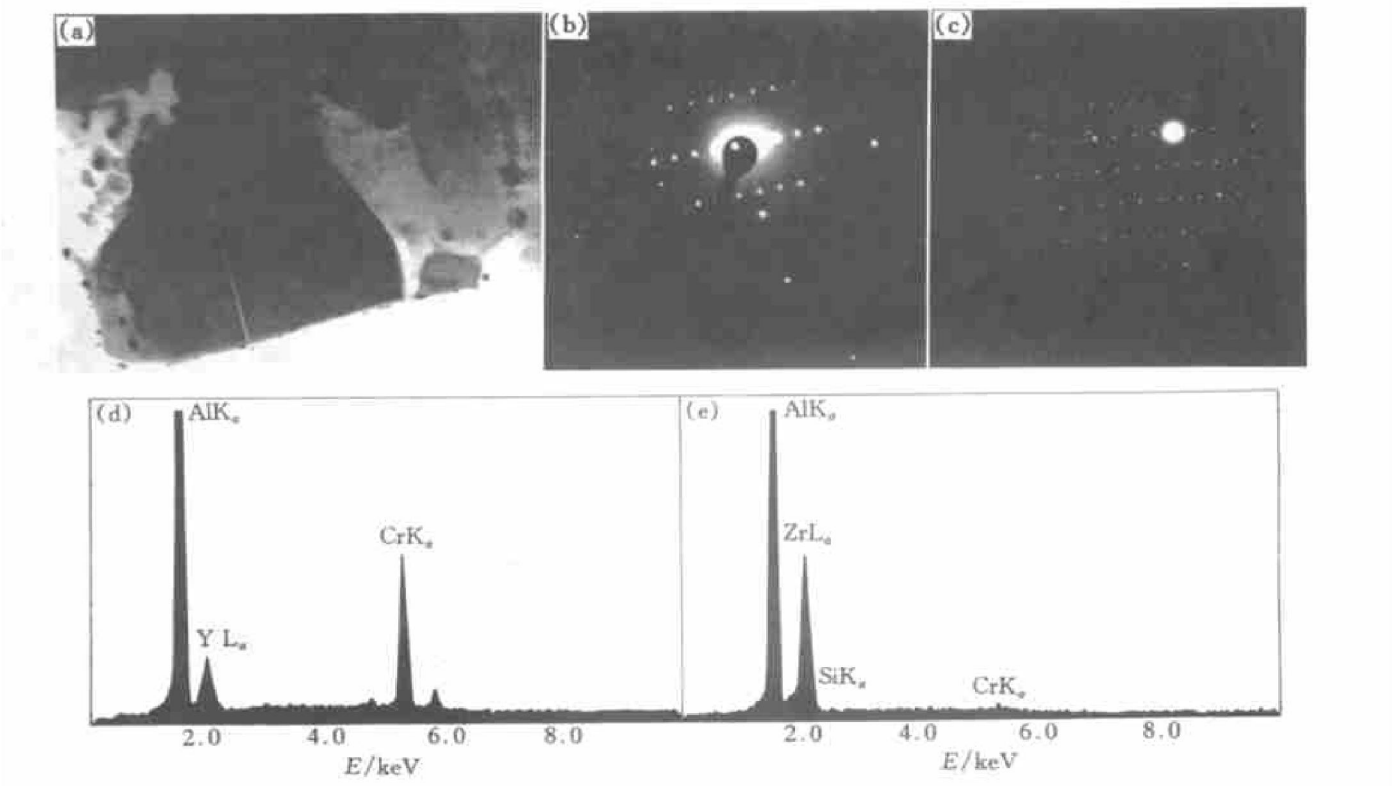

Fig. 6 Energy spectra and select area diffraction patterns from second phases
(a) —TEM morphology, exposed at 550 ℃ for 32 h; (b) —SAD, $Al_{20}Cr_2Y$; (c) —SAD, DO_{23} Al_3Zr;
(d) —Energy spectrum of $Al_{20}Cr_2Y$; (e) —Energy spectrum of DO_{23} Al_3Zr

alloy, perhaps has more satisfied mechanical properties and heat-resistance.

4 CONCLUSIONS

1) Main second phases, precipitated from rapidly solidified Al-5.0Cr-4.0Y-1.5Zr alloy during thermal exposure, are identified as cubic $Al_{20}Cr_2Y$ with lattice parameter of 1.437 nm, instead of $Al_{13}Cr_2$, and metastable Ll_2 Al_3Zr or equilibrium DO_{23} Al_3Zr. The cubic dispersion precipitates prior to the two other Al_3Zr type intermetallic phases in the course of the decomposition of supersaturated solid solution.

2) The precipitation of $Al_{20}Cr_2Y$ will lead to reduction of the hardness of the foil powder due to incoherence nature of $Al_{20}Cr_2Y$ precipitate. Ll_2 Al_3Zr has

intensive precipitation strengthening effect, but Al_3Zr will transform into DO_{23} from Ll_2 structure during thermal exposure above 550 ℃.

3) The $Al_{20}Cr_2Y$ phase is structurally stable and maintain its cubic structure up to 600 ℃, but it is prone to coarsen and polygonize at the temperature higher than 450 ℃. Both stable DO_{23} Al_3Zr and metastable Ll_2 Al_3Zr precipitates have much smaller coarsening rate than $Al_{20}Cr_2Y$ above 450 ℃, and they are able to keep their fine spherical morphologies up to 550 ℃.

[REFERENCES]

[1] Marshall G J, Hughes I R, Miller W S. Effect of consolidation route on structure and property control in rapidly solidified Al-Cr-Zr-Mn powder alloy for high temperature service [J]. Materials Science and Technology, 1986, 2(4): 394- 399.

[2] Marshall G J, Ioannidis E K. Influence of rapid solidification route on microstructure and properties of a thermally stable Al-Cr-Zr-Mn alloy [J]. Journal of Materials Science, 1992, 27(2): 3552- 3564.

[3] Zedalis M S, Fine M E. Precipitation and Ostwald ripening in the dilute Al based-Zr-V alloys [J]. Metallurgical Transaction, 1986, 17A(10): 2187- 2195.

[4] Chuang M S, Tu G C, Shimizu K. Effect of Nb-addition on the thermal stability of rapidly solidified Al-Cr-Zr alloys [J]. Light Metals, (in Japanese), 1995, 45(9): 497- 503.

[5] Lieblich M, Laruana G, Torralba M, et al. Characteristics of Al-Cr-Zr alloy powders made by confined nozzle atomization [J]. Materials Science and Technology, 1996, 12(1): 25- 33.

[6] Hawk J A, Angers L M, Wilsdorf H G F. Dispersion strengthened aluminum alloys [A]. Kim Y W, Griffith W M. The Minerals, Metals & Materials Society TMS-AIME [C]. Warrendale, PA, 1988. 339- 346.

[7] Mahajam Y R, Kirchoff S D, Froes F H. Thermal stability of rapidly solidified Al-Ti-Gd alloy [J]. Scripta Meterialia, 1986, 20(5): 643- 647.

[8] Saunder N, Rivilin V G. Critical assessment: thermodynamic characterization of Al-Cr, Al-Zr, and Al-Cr-Zr alloy systems [J]. Materials Science and Technology, 1986, 2(5): 521- 527.

[9] XIAO Yu-de, LI Song-rui, XIE Yun-an, et al. Microstructure and decomposition of rapidly solidified Al-Fe-Cr-Zr alloy [J]. Trans Nonferrous Met Soc China, 1994, 4(4): 109- 113.

[10] TANG R Z. Foundation of Physics Metallurgy [M]. Beijing: Metallurgical Industry Press, 1997(8). 52.

[11] XIAO J M. Alloy Phase and Phase Transformation [M], (in Chinese). Beijing: Metallurgical Industry Press, 1986(7). 92.

[12] You B S, Park W W. Age hardening phenomena and microstructures of rapidly solidified Al-Ti-Si and Al-Cr-Y alloys [J]. Scripta Meterialia, 1996, 34(2): 201- 205.

(Edited by HUANG Jin-song)